SLAC-PUB-11924
June 2006

Reflectivity Measurements for Copper and Aluminum in the Far Infrared and the Resistive Wall Impedance in the LCLS Undulator *

K.L.F. Bane, G. Stupakov, SLAC, Stanford, CA 94309
J.J. Tu, Department of Physics, The City College of New York, New York, NY 10031

Reflectivity measurements in the far infrared, performed on aluminum and copper samples, are presented and analyzed. Over a frequency range of interest for the LCLS bunch, the data is fit to the free-electron model, and to one including the anomalous skin effect. The models fit well, yielding parameters dc conductivity and relaxation times that are within 30-40% of expected values. We show that the induced energy in the LCLS undulator region is relatively insensitive to variations on this order, and thus we can have confidence that the wake effect will be close to what is expected.

Presented at the European Particle Accelerator Conference (EPAC 06), Edinburgh, Scotland, June 26-30, 2006

*Work supported by Department of Energy contract DE–AC02–76SF00515.

Reflectivity Measurements for Copper and Aluminum in the Far Infrared and the Resistive Wall Impedance in the LCLS Undulator *

K.L.F. Bane, G. Stupakov, SLAC, Stanford, CA 94309
J.J. Tu, Department of Physics, The City College of New York, New York, NY 10031

Abstract

Reflectivity measurements in the far infrared, performed on aluminum and copper samples, are presented and analyzed. Over a frequency range of interest for the LCLS bunch, the data is fit to the free-electron model, and to one including the anomalous skin effect. The models fit well, yielding parameters dc conductivity and relaxation times that are within 30-40% of expected values. We show that the induced energy in the LCLS undulator region is relatively insensitive to variations on this order, and thus we can have confidence that the wake effect will be close to what is expected.

INTRODUCTION

In the Linac Coherent Light Source (LCLS) [1], longitudinal wakefields generated in the undulator region induce an energy variation along the bunch that will affect the performance of the FEL. The largest wake contributor in this region is the resistive wall wakefield of the beam pipe. In the undulator region the LCLS bunch is short (the rms length $\sigma_z = 20$ μm), and the shape can be described as uniform, but with "horns" of charge at the head and tail. For such high bunch frequencies, the resistive wall wake derived from a free-electron model of conductivity, including the frequency dependence of conductivity, has been deemed an appropriate model to use [2]. A question that comes to mind is, How valid is such a model for the LCLS beam pipe?

Reflectivity measurements have long been used to study electrical properties of metals as functions of frequency. Our range of interest is wave number $k = 0.06$–0.6 μm^{-1}. Unfortunately, reflectivity measurements work best at frequencies higher than these (in this range the reflectivity of good metals is very near 1), and in the literature, over this range, little data can be found. For aluminum (copper), for example, the published data reaches only down to $k = 0.2$ (0.3) μm^{-1} [3,4]. Therefore, it was decided to take Al and Cu samples, produced at Argonne National Lab, and to perform reflectivity measurements, to see how well—over our frequency range of interest—the free-electron model with the accepted parameters holds.

In this report we describe reflectivity at normal incidence measurements performed by one of us (JT) at the Physics Department of Brookhaven National Laboratory, analyze the results, and discuss the implications for the LCLS.

* Work supported by the Department of Energy, contract DE-AC02-76SF00515

REFLECTIVITY AND THE FREE-ELECTRON MODEL

Unlike the case of polarized radiation at oblique angles, with normal incidence phase information is lost. In principle, this can be regained by measuring to the plasma frequency k_p (for Cu $k_p \approx 50$ μm^{-1}) and then using Kramers-Kronig integrals; in this way a complex index of refraction $\tilde{n}(k)$ or conductivity $\tilde{\sigma}(k)$ can be found (see *e.g.* Ref. [5]). Here we are interested only in the very low frequency part of the data, where presumably the free-electron model applies; we will thus directly fit the free-electron model to the low frequency end of the data.

Equations that relate reflectivity R with the free-electron parameters dc conductivity σ and relaxation time τ are:

$$\tilde{\sigma} = \frac{\sigma}{1 - ikc\tau} \ , \tag{1}$$

$$\tilde{n} = \sqrt{\tilde{\epsilon}} = \sqrt{1 + \frac{4\pi i\tilde{\sigma}}{kc}} \ , \tag{2}$$

$$R = \left| \frac{\tilde{n} - 1}{\tilde{n} + 1} \right|^2 \ , \tag{3}$$

with $\tilde{\sigma}$ ac conductivity, $\tilde{n}$ index of refraction, $\tilde{\epsilon}$ dielectric constant, c the speed of light. We work in Gaussian units.

In Fig. 1 we show the ideal behavior of R for a reasonably good conducting metal, where $\sigma = 0.12 \times 10^{17}$/s and $\tau = 0.55 \times 10^{-14}$ s (solid line); these parameters are, respectively, 2% (σ) and 20% (τ) of the nominal values for copper. The parameters were chosen so that the important features of $R(k)$ could be seen easily in one plot. We see three distinct regions: (1) for low frequencies, $k \lesssim 1/c\tau$, R continually decreases, with positive curvature, and with a low frequency asymptote of $(1 - \sqrt{2kc/\pi\sigma})$; (2) for intermediate frequencies the reflectivity is nearly constant, $R \approx (1 - \sqrt{1/\pi\sigma\tau})$; (3) for $k \gtrsim k_p = \sqrt{4\pi\sigma/c^2\tau}$, R quickly drops to zero. The dashed lines in Fig. 1 give the analytic guideposts for the 3 regions.

Note that it is only in the first and the beginning of the second region that we can expect the free-electron model to have validity in real metals; at higher frequencies the effects of absorption bands and other physics will distort the $R(k)$ curve. In principle, knowing R accurately in the entire 1st region suffices for obtaining the free-electron parameters σ and τ; in practise, however, knowing it also in the 2nd region gives us more confidence in the model and especially in the value of τ.

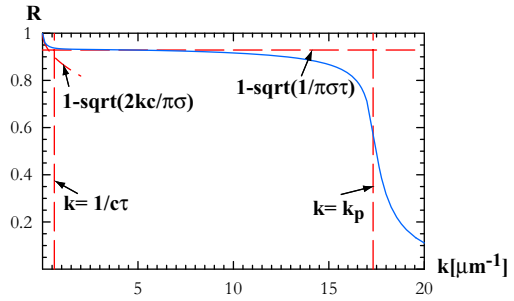

Figure 1: Reflectivity R *vs.* frequency k for an ideal conductor, assuming the free-electron model (solid line). Analytic guideposts are also given (dashes).

Anomalous Skin Effect (ASE)

When the skin depth δ_{rw} becomes less than or comparable to the mean free-path of electrons ℓ the classical ac model of conductivity no longer holds, and the (room temperature) anomalous skin effect (ASE) applies [6, 7]. [For Cu, $\delta_{rw} \approx \ell$ when $k = (20\ \mu\text{m})^{-1}$.] Different expression are known for the cases of *specular* and *diffuse* reflection of electrons at the surface. Fitting these formulas to infrared measurements for Cu, Ag, Au, Lenham and Treherne concluded that the diffuse model is normally applicable, even for well-prepared samples [4]. This is the model we use.

For diffuse reflection, the surface impedance is [7]

$$Z_s = \frac{4\pi i k\tau}{1+ikc\tau}\sqrt{\frac{\Lambda}{3\pi\tau\sigma}}\, I_0^{-1}\!\left(\frac{ikc\tau\Lambda}{(1+ikc\tau)^3}\right)\,, \quad (4)$$

$$I_0(\xi) = \frac{1}{\pi}\int_0^\infty \ln\left(1+\frac{\xi\kappa(t)}{t^2}\right)dt\,, \quad (5)$$

$$\kappa(t) = \frac{2}{t^3}\left[(1+t^2)\tan^{-1}t - t\right]\,, \quad (6)$$

with ASE parameter $\Lambda = 3\pi\ell^2\sigma/c^2\tau$. Then $\tilde{n} = 4\pi/Z_s^* c$.

For given σ, τ, ASE's effect on $R(k)$ will be small in the lowest energy region (region 1); in region 2 (the flat region), $R(k)$ will be lower than for the classical, ac model.

MEASUREMENTS

Three samples were measured: an Al film, solid Al, and solid Cu. The samples (thickness $\sim$ few mm) were mounted on an optically-black cone, and the room temperature reflectivity was measured in a near-normal-incidence arrangement from $k \sim 0.02$–$10\ \mu\text{m}^{-1}$ on a Bruker IFS 66v/S and a Bruker IFS 113v Fourier transform infrared (FTIR) spectrometer. By evaporating a thick gold film in situ in ultra-high vacuum ($< 1\times10^{-8}$ Torr) over the sample, the precise ratio of sample reflectivity to the reflectivity of Au was measured. Knowing the reflectivity of Au, the absolute reflectivity of the sample was thus determined. The details of this technique have been described previously [8–10]. Using this in situ evaporation technique, the errors associated with misalignments, window interference and surface inhomogeneity can be eliminated. As a result, absolute reflectivity of the sample $R(k)$ can be measured to a precision of 0.1% or better.

Fig. 2 shows $R(k)$ for Cu and evaporated Al over the entire measured range. [The solid Al sample is considered a bad sample: it had poor reflectivity ($R = 0.95$ at $k = 0.5\ \mu\text{m}^{-1}$) and noticeable granularity. This sample's data is considered no further.] Comparing the general features of the data with the literature, we see for Cu the onset to interband absorption at $10\ \mu\text{m}^{-1}$ as in Ref. [11] (p. 297), for Al a weakly suggested absorption spike at $7.5\ \mu\text{m}^{-1}$ that is very pronounced in Ref. [5]. For Cu, the dip beginning at $1.5\ \mu\text{m}^{-1}$ is not seen in Ref. [11]. We assume the differences are due to sample variability (finish, etc).

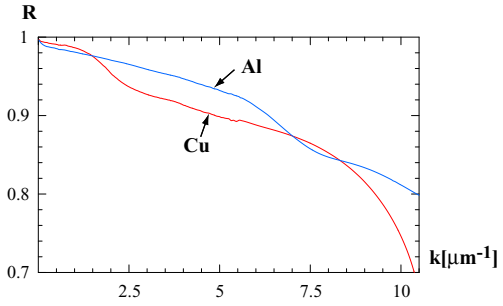

Figure 2: Measurement results: Reflectivity R *vs.* frequency k for copper and evaporated aluminum.

Focusing on frequencies below $1\ \mu\text{m}^{-1}$: we see in R a possibly correct dependence at the very low end [$(1-R) \sim \sqrt{k}$]. But this is followed, unexpectedly, by a linear decrease (not a constant). When comparing the Al curve with reflectivity measurements performed in 1980 by Shiles, *et al* [5], we can see that the earlier measurements also have a slope, but that is a factor of 2 less steep. The non-zero slope is not understood. The data is, nevertheless, smooth and well-behaved at low k, to $0.5\ \mu\text{m}^{-1}$ for Al, to $0.3\ \mu\text{m}^{-1}$ for Cu (representing, respectively, 85% and 50% of our range of interest). We assume our models are valid in these regions, and in these regions we will perform our fits.

Fitting to the Data

The aluminum comparison, over nearly twice the region of interest, is given in Fig. 3. Blue repeats the measured results. The result of the nominal free-electron model, with $\sigma = 3.35\times10^{17}$/s and $\tau = 0.75\times10^{-14}$ s (at 295 K) [11], is given in green. The fit to the ac model (the red curve) gives parameters, relative to their nominal values: $\sigma_r = 0.63$, $\tau_r = 0.78$. The fit to the ASE model ($\ell = 0.016\ \mu$m; the dashed curve) gives: $\sigma_r = 0.61$, $\tau_r = 1.28$. We note that the fitted curves fit the data very well up to $0.5\ \mu\text{m}^{-1}$, that σ is less than ideal by a factor of 2/3 (which is plausible), and that τ is near nominal. Note that the ASE model, which differs from the ac model only when k is not too small, gives a fit that is unique only in τ.

The copper comparison is shown in Fig. 4. Given are the measured data (blue) and the nominal calculation, with $\sigma =$

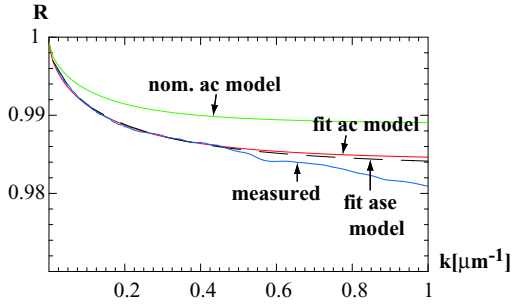

Figure 3: Aluminum reflectivity: comparison of measurements (blue) with calculations using nominal (green) and fitted ac models (red), and the fitted ASE model (dashes).

5.26×10^{17}/s and $\tau = 2.52\times10^{-14}$ s (at 295 K; green) [11]. The fit to the ac model (the red curve) gives: $\sigma_r = 0.66$, $\tau_r = 0.67$. The fit to the ASE model ($\ell = 0.039$ μm; the dashed curve) gives: $\sigma_r = 0.70$, $\tau_r = 1.28$. We again see agreement at the very low frequency end of the plot up to 0.25 $\mu\mathrm{m}^{-1}$, though the data is less smooth then before. Note that in this case the agreement breaks down far below the upper end of the desired frequency range (0.6 $\mu\mathrm{m}^{-1}$). All fitting results are summarized in Table 1.

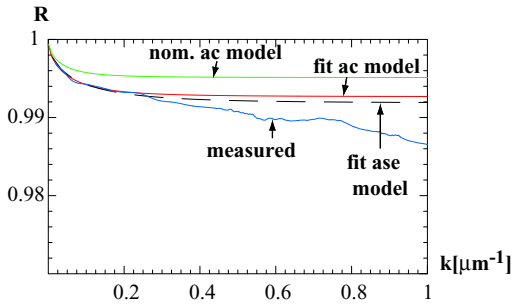

Figure 4: Copper reflectivity: comparison of measurements (blue) with calculations using nominal (green) and fitted ac models (red), and the fitted ASE model (dashes).

Table 1: Fitted parameters, relative to their nominal values, assuming the ac model (f_{ac}) and the ASE model (f_{ase}).

Sample	Nominal values	f_{ac}	f_{ase}
Al	$\sigma = 3.35\times10^{17}$ s^{-1}	0.63	0.61
	$\tau = 0.75\times10^{-14}$ s	0.78	1.28
Cu	$\sigma = 5.26\times10^{17}$ s^{-1}	0.66	0.70
	$\tau = 2.52\times10^{-14}$ s	0.67	1.28

IMPLICATIONS FOR THE LCLS

The LCLS undulator beam pipe will be plated with Al, in cross-section will be primarily flat (*spec.* rectangular, with aperture horizontal 10 mm by vertical 5 mm). The impedance of a purely flat vacuum chamber is given by [2]

$$Z(k) = \frac{1}{c}\int_{-\infty}^{\infty} \frac{dq}{\cosh(qa)[\tilde{n}(k)\cosh(qa) - \frac{ik}{q}\sinh(qa)]} \,. \quad (7)$$

Inverse Fourier transforming $Z(k)$ we obtain the point charge wake. Finally, convolving with the bunch shape we obtain the induced relative energy variation $\Delta E/E$. In Fig. 5 we plot the numerically obtained $\Delta E/E$ for the three Al models discussed above; the bunch shape λ_z is also superimposed. Here bunch charge is 1 nC, energy 14 GeV; beam pipe length is 130 m and aperture 5 mm. We see that the three results are very similar.

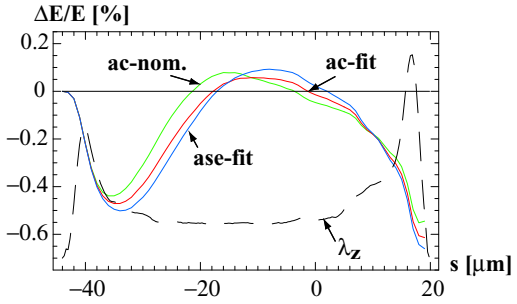

Figure 5: Energy spread induced in the LCLS undulator region for the different models, assuming a flat, Al beam pipe. The bunch shape λ_z is also shown (head to the left).

In a SASE FEL the energy variation induced in the beam in the undulator region needs to be limited to a few times the Pierce parameter, in the LCLS to $\sim 0.3\%$; particles outside such an energy window will not reach saturation. We note that the horns in the LCLS beam induce a large energy variation. We note also that in the cases nominal, ac fit, ASE fit, a maximum of 51%, 51%, 47% of the beam falls within a 0.3% energy window. Thus, for optimizing the fraction of beam that will lase, all three cases are essentially equivalent.

We conclude that for LCLS beam parameters we are relative insensitive to which model (ac or ASE) applies, and to parameter variations of 30-40%. This means that we can have confidence that the resistive wall wake effect in the undulator region will be close to what has been expected.

We thank J. Welch for helpful discussions on this topic.

REFERENCES

[1] LCLS-CDR, SLAC Report No. SLAC-R-593, 2002.

[2] K. Bane and G. Stupakov, PAC05, 3390 (2005).

[3] M. Ordal et al., Applied Optics **22**, 1099 (1983).

[4] A. P. Lenham, D. M. Treherne, J Opt Soc Am **55**, 683 (1966).

[5] E. Shiles et al., Physical Review B **22**, 1612 (1980).

[6] C. Reuter, E. Sondheimer, Proc Roy Soc A **195**, 336 (1947).

[7] R. B. Dingle, Physica **19**, 311 (1953).

[8] C. C. Holmes et al., Appl Opt **32**, 2972 (1993).

[9] J. J. Tu et al., Phys Rev Lett **87**, 277001 (2001).

[10] J. J. Tu et al., Phys Rev B **66**, 144514 (2002).

[11] N. Ashcroft and N. Mermin, *Solid State Physics* (Harcourt Brace College Publishers, Orlando, FL, 1976).